Pergamon

Electrochimica Acta, Vol. 41, No. 4, pp. 533–541, 1996
Elsevier Science Ltd.
Printed in Great Britain
0013-4686/96 $15.00 + 0.00

0013-4686(95)00340-1

THE REMOVAL OF Pb(II) FROM AQUEOUS SOLUTIONS USING A RETICULATED VITREOUS CARBON CATHODE CELL—THE INFLUENCE OF THE ELECTROLYTE MEDIUM*

C. PONCE DE LEON and D. PLETCHER†
Department of Chemistry, The University, Southampton SO17 1BJ, England, UK.†

(*Received* 25 *October* 1994)

Abstract—The removal of Pb(II) ions from aqueous solutions of perchlorate, nitrate, tetrafluoroborate, chloride and sulfate, pH 2, has been investigated in a cell with a reticulated vitreous carbon cathode. It is confirmed that the Pb(II) may always be removed. There are, however, marked differences in the conditions necessary and the performance attained by the system (*eg*, rate of removal, current efficiency), even with these nominally similar, aqueous acid media. The origin of these differences are investigated.

Key words: three dimensional electrodes, effluent treatment reduction of Pb(II).

1. INTRODUCTION

There remains a high level of interest in technology for removing transition and heavy metals from effluents, waters and process streams to levels $\ll 1$ ppm. For at least 30 years, there has been a recognition that electrolytic methods can achieve these goals. Indeed, a number of commercial systems, based on three dimensional electrodes, rotating cylinders *etc.*, are now marketed and applied to the removal of several metal ions including Ag(I), Cu(II), Pb(II), Zn(II), Cd(II), Hg(II) and Ni(II)[1–5]. Perusal of these reviews shows that there is also a substantial literature but most of the academic studies have emphasised the design of reactors, the performance of various electrodes and mass transport correlations; hence, typically, the experiments have used model solutions where metal deposition is always mass transport controlled. In consequence, although they are common in the real world, there is little information available about systems where chemical or electrochemical complications make the behaviour of the cell less ideal.

We have therefore become interested in investigating the influence of chemical and electrochemical complications on the performance of metal ion removal cells. In this paper, we report studies of lead recovery from a series of solutions (perchlorate, nitrate, tetrafluoroborate, chloride and sulfate) all at pH 2 and demonstrate that even in such nominally similar solutions, complications can arise.

The experiments employ a membrane cell with a reticulated vitreous carbon cathode operating in the flow-by mode. Reticulated vitreous carbon is an open pore material with a honeycomb structure, composed of vitreous carbon; it is chosen as the electrode material because of its high surface area, high porosity, high isotropic electrical conductivity, rigid structure and inertness both on open circuit and over a wide potential range in many aqueous media[6]. It is also available commercially in several porosity grades from 10 to 100 pores per inch (ppi). Reticulated vitreous carbon has previously been used for electroanalytical purposes[7–14] including the deposition of metal for preconcentration. Pletcher *et al.*[15–18] have also characterised mass transport in the cell used here and described its application to the removal of copper (II) from a sulfate medium, pH 2. Recently, Tissot *et al.*[19] electrodeposited PbO_2 on reticulated vitreous carbon and used the electrode for the direct oxidation of CN^-.

2. EXPERIMENTAL

The cell and flow circuit have previously been described in detail[15, 20]. The reticulated vitreous carbon cathodes (50 mm × 50 mm × 12 mm thick) were cut from blocks supplied by the Electrosynthesis Co and they fitted tightly into the centre of the catholyte channel between the membrane and the steel current collector to which contact was made with conducting carbon cement (Leit-C from Agar Aids). The Luggin capillary was a small plastic tube inserted through a 3 mm hole drilled through the steel current collector; the tip of the tube was positioned ≈ 2 mm into the reticulated vitreous carbon structure and usually the reference electrode was a Radiometer type K401 saturated calomel electrode. In experiments where chloride contamination was a concern, the reference electrode was a mercury/mercury sulfate electrode prepared in the laboratory with saturated potassium sulfate.

* This paper is dedicated to Professor Frank Goodridge on the occasion of his retirement from the University of Newcastle.

† Author to whom correspondence should be addressed.

All solutions were prepared with water from a Milli-Ro 15/Milli-Q purification system and chemicals of the highest grade available, usually Analar reagents. In all cases, solutions were 0.5 M in the appropriate sodium salt adjusted to pH 2 with the corresponding acid. Except where otherwise stated, the lead was added to the solution as the salt with the common anion.

Pb(II) concentrations were determined by atomic absorption spectroscopy using a Perkin Elmer 2380PE model 157 spectrometer with an oxygen/acetylene flame. Standard solutions were prepared by dilution with the appropriate electrolyte of a standard, Spectrosol 1000 ppm Pb(II) solution.

3. RESULTS

3.1 *Voltammetry in the reticulated vitreous carbon cell*

Current, I, vs. potential, E, curves were recorded for deoxygenated, dilute solutions of Pb(II) in each of the media, pH 2 using a 60 ppi reticulated vitreous carbon electrode. In each medium, the influence of flow rate was studied and in some cases 10 ppi and 100 ppi reticulated vitreous carbon were also used.

3.1.1 *Chloride.* Figure 1 reports I–E curves for a solution of 7 ppm (34 μM) Pb(II) in 0.5 M NaCl, pH 2, recorded at 10 ppi and 100 ppi reticulated vitreous carbon electrodes. It can be seen that at both materials, well formed reduction waves are observed with $E_{1/2} \approx -0.64$ V. The foot of the waves are very steep, reflecting the need for a nucleation overpotential to commence the deposition of lead on the carbon surface, and the limiting current plateaux are clearly defined and strongly dependent on the solution velocity. The reverse scans (not shown) show the same limiting currents as the forward scans but there is a narrow potential range between approximately -0.60 V and -0.50 V where the cathodic current is higher on the reverse scan and, at slightly more positive potentials, there is a large, symmetrical anodic peak for the redissolution of the lead from the surface; these characteristics are typical of those for simple metal deposition and dissolution reactions on a carbon surface.

It would appear that, in the plateaux region, the current for Pb(II) reduction is mass transfer controlled. Hence, using the simplest model for the three dimensional electrode where its whole surface is operating under mass transfer control and there is no significant depletion of the reactant through the electrode, the limiting current, I_L, is given by the equation

$$I_L = -nFk_m A_e V_e c \qquad (1)$$

where k_m (m s^{-1}) is the mass transfer coefficient and A_e (m^2 m^{-3}) is the specific area of the reticulated vitreous carbon, V_e the volume of the cathode, c the concentration of Pb(II) (mol m^{-3}), F the Faraday constant and, here, $n = 2$. This equation was used to estimate values of $k_m A_e$ at each flow velocity, v, using limiting currents determined both from I–E curves such as those shown in Fig. 1 and from experiments carried out at constant potential. The data are presented in Fig. 2. The best fit correlation equations for the three grades of reticulated vitreous

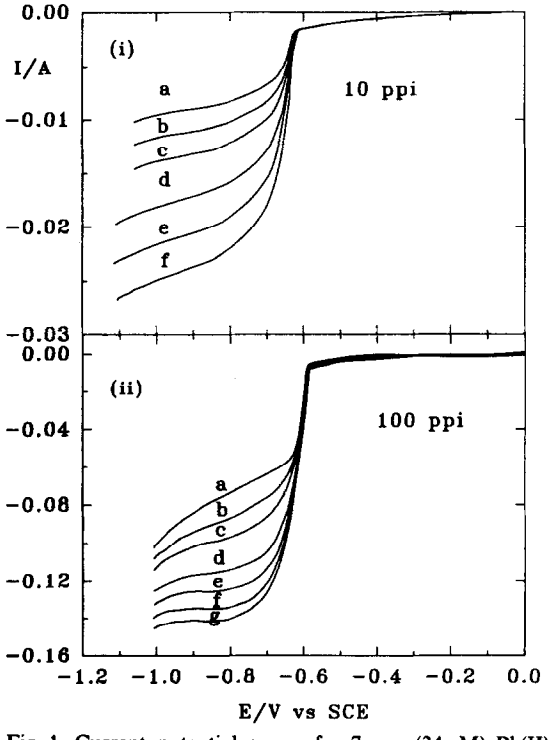

Fig. 1. Current–potential curves for 7 ppm (34 μM) Pb(II) in 0.5 M NaCl at pH 2. Reticulated vitreous carbon cathodes (i) 10 ppi (ii) 100 ppi. The linear flow velocities are (a) 0.016 (b) 0.030 (c) 0.045 (d) 0.088 (e) 0.13 (f) 0.16 (g) 0.21 m s^{-1}. Potential scan rate 5 mV s^{-1}. Temperature 298 K.

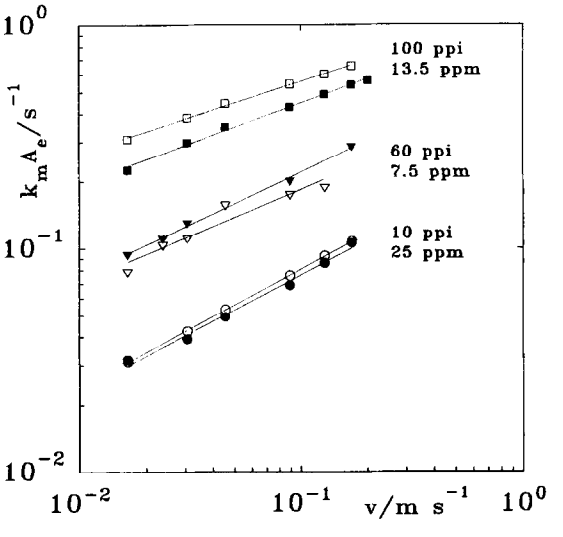

Fig. 2. Plots of $k_m A_e$ vs. the linear flow velocity, v, for solutions of Pb(II) in 0.5 M NaCl at pH 2. Reticulated vitreous carbon cathodes. The open symbols use data from the limiting current region of I–E curves similar to those shown in Fig. 1. The shaded symbols report data from experiments where the potential was held constant at a value in the limiting current region and the linear flow velocity was changed. Temperature 298 K.

carbon are:

$$10 \text{ ppi} \quad k_m A_e = 0.24 v^{0.50}$$

$$60 \text{ ppi} \quad k_m A_e = 0.57 v^{0.45}$$

$$100 \text{ ppi} \quad k_m A_e = 1.08 v^{0.35}$$

It can be seen that $k_m A_e$ increases with the number of ppi, while the velocity exponents indicate only slight deviations from laminar flow. These data, together with the characteristics in Table 1, were used to construct plots of Sherwood number vs. Reynolds number. The values of the specific surface areas are those reported by Whyte[15, 21] although similar values are reported elsewhere[22, 23]. Figure 3(a) reports the data from the experiments using Pb(II) reduction in 0.5 M NaCl solution at the three grades of reticulated vitreous carbon and, since there is no significant difference with the grade of reticulated vitreous carbon, a single correlation line is drawn through the data. The figure also shows a similar correlation line drawn by Whyte[15, 21] from experiments on the reduction of Cu(II). The agreement is quite acceptable and our data confirm that the enhancement in performance of reticulated vitreous carbons in electrolytic cells with increase in the number of ppi are almost entirely the result of the increased surface area; foam material appear to be poor turbulence promoters as has been pointed out by several recent papers[15, 25, 26]. Figure 3(b) compares Sherwood number vs. Reynolds number plots for the reduction of ferricyanide, copper (II) and lead (II) at 10 ppi reticulated vitreous carbon and again a very satisfactory agreement is observed. Both Figs 3(a) and 3(b) confirm that the reduction of Pb(II) in the chloride medium is mass transport controlled.

3.1.2 *Nitrate.* When *I–E* curves were recorded at the reticulated vitreous carbon electrodes for solutions of Pb(II) in 0.5 M sodium nitrate, pH 2, the results were markedly different. Figure 4 shows a typical set of curves recorded at a 60 ppi electrode for a 20 ppm Pb(II) solution. On the forward scan, the reduction wave for the reaction $Pb(II) \rightarrow Pb$ occurs at $E_{1/2} \approx -0.66$ V. The wave is drawn out and the limiting current plateau is only very poorly defined; there is a marked tendency for the current to continue to increase as the potential is made more negative. On the reverse scan, the limiting current plateaux appear better defined and the reduction wave is steeper. At more positive potentials a sharp anodic stripping peak is again observed. Such responses suggest slow steps in the nucleation and/or early stages of growth of the lead metal on the carbon surface; the back scan would then reflect the curve at a surface already covered by some lead. Even on the back scan, however, the limiting currents themselves were smaller than expected for a mass transport controlled reaction by (25–40%) and their variations with electrolyte velocity were less than expected. Clearly, the deposition of lead onto reticulated vitreous carbon from nitrate in these conditions is not fully mass transport controlled. Furthermore, when this or similar sets of experiments were repeated over a period of days, the curves were not completely reproducible. On some occasions,

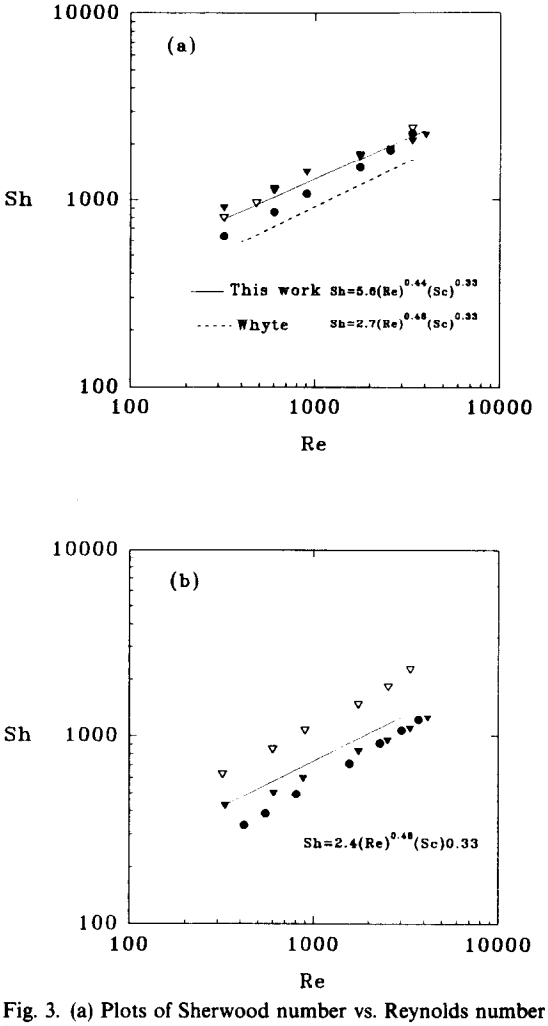

Fig. 3. (a) Plots of Sherwood number vs. Reynolds number for solutions of Pb(II) in 0.5 M NaCl at pH 2. (●) 10 ppi, (▼) 60 ppi, (▽) 100 ppi. The solid line is the "best fit line" to the data at all three grades of reticulated vitreous carbon. The dashed line is the "best fit line" to data for the reduction of Cu(II) in Na_2SO_4, pH 2 at all three grades of reticulated vitreous carbon, as reported by Whyte *et al.*[15, 21]. Temperature 298 K. (b) Plots of Sherwood number vs. Reynolds number at a 10 ppi reticulated vitreous carbon cathode for solutions of: (●) Cu(II) in Na_2SO_4, pH 2, (▼) $Fe(CN)_6^{3-}$ in 0.2 M NaOH, (▽) Pb(II) in 0.5 M NaCl at pH 2. The solid line is the "best fit line" to the data for all three solution. Temperature 298 K.

Table 1. Characteristics and properties used in the Sherwood and Reynolds numbers

Properties of 0.5 M NaCl	
Relative density	1018.9 kg m^{-3}
Dynamic viscosity	$0.001\,05 \text{ kg m}^{-1} \text{s}^{-1}$
Diffusion coefficient of Pb(II) in 0.5 M NaCl	$7 \times 10^{-10} \text{ m}^2 \text{s}^{-1}$
Characteristic diameter of cell	0.0193 m
Specific surface areas	
10 ppi	$1300 \text{ m}^2 \text{m}^{-3}$
60 ppi	$2400 \text{ m}^2 \text{m}^{-3}$
100 ppi	$6700 \text{ m}^2 \text{m}^{-3}$

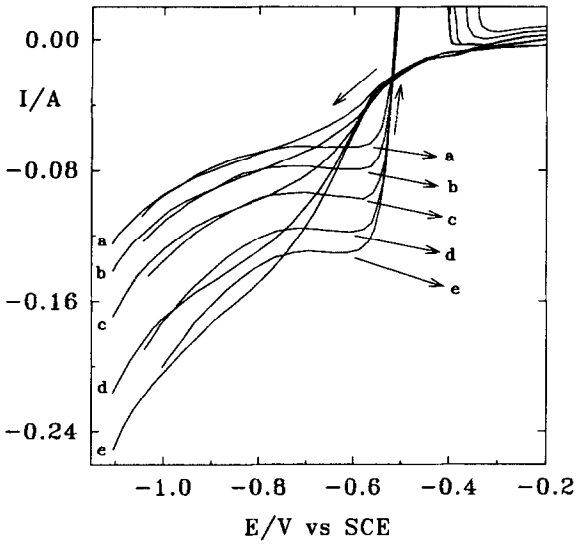

Fig. 4. Current–potential curves for 20 ppm Pb(II) in 0.5 M $NaNO_3$ at pH 2 at a 10 ppi reticulated vitreous carbon cathode. The linear flow velocities are (a) 0.045, (b) 0.088, (c) 0.13, (d) 0.17, (e) 0.21 m s^{-1}. Potential scan rate 5 mV s^{-1}. Temperature 298 K.

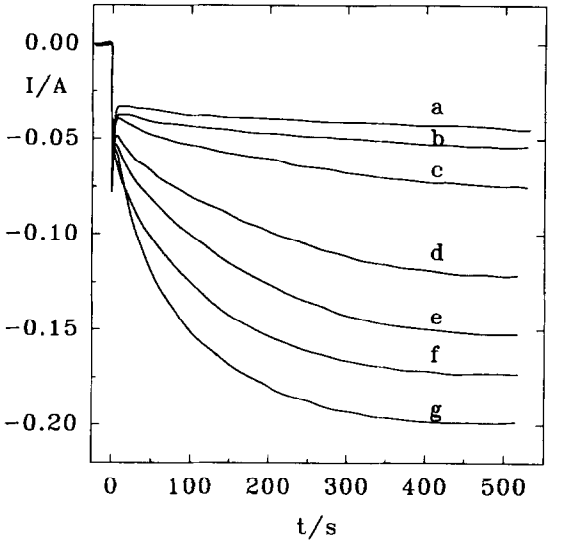

Fig. 5. Current–time responses to a potential step from −0.2 V to −0.6 V vs. *sce* for 100 ppm Pb(II) in 0.5 M $NaNO_3$ at pH 2 at a 10 ppi reticulated vitreous carbon cathode. The linear flow velocities are (a) 0.016, (b) 0.031, (c) 0.045, (d) 0.080, (e) 0.13, (f) 0.17, (g) 0.21 m s^{-1}. Temperature 298 K.

little lead deposition was observed during a scan but usually there are variations in the shape of the wave on the forward scan and the magnitudes of the limiting currents (and their variation with electrolyte velocity) on the reverse scan. Such behaviour also suggests that it is the nucleation and early stages of growth of the lead which are not reproducible. This could result from variations in the surface of the reticulated vitreous carbon with history and pretreatment or from the formation of partially passivating layers, *eg*, insoluble Pb(II) species during some of the experiment.

Figure 5 reports the current as a function of time, when the potential of the reticulated vitreous carbon electrode was stepped from −0.2 V vs. *sce* to −0.6 V (a potential within the plateau region on the reverse scans of Fig. 4) in a solution containing 100 ppm Pb(II) in 0.5 M $NaNO_3$, pH 2. It can be seen that at each flow rate, the cathodic current increases with time over a period of several hundred seconds and that the steady state currents are strongly dependent on electrolyte velocity. After several hundred seconds, however, the charge passed is sufficient that the surface should be fully covered by lead metal. In this context, it should also be noted that the *I–E* curves discussed above involve a shorter period of lead deposition and, hence, do not reflect the steady state situation. Certainly, *I–t* transients where the cathodic current increases with time are usually an indication that the active surface area for metal deposition is increasing and commonly that the kinetics of nucleation and phase growth kinetics are important. When such potential step experiments are carried out in chloride media, the steady state current is reached within 10 s.

3.1.3 *Perchlorate and tetrafluoroborate. I–E* curves for solutions of Pb(II) in sodium perchlorate, pH 2, and sodium tetrafluoroborate, pH 2, showed similar characteristics to those in the nitrate medium. On the forward scans, the reduction waves are poorly formed and drawn out and, although the reverse scans generally showed limiting current plateaux, the currents were not as large as expected for mass transport control and they showed only a low dependence on the electrolyte velocity. Moreover, reproducibility was again a problem. Since lead tetrafluoroborate was not available, in this medium solutions were prepared by dissolution of the metal in HBF_4 as well as by dissolving lead nitrate and lead chloride. This led to the interesting observation that, when the solutions were prepared from lead chloride, the shape of the curves as well as their reproducibility improved substantially. This suggests that even trace quantities of chloride could catalyse the deposition of lead, perhaps by adsorption on the reticulated vitreous carbon surface.

3.1.4 *Sulfate.* Figure 6 illustrates a *I–E* curve for a saturated solution of $PbSO_4$ in Na_2SO_4, pH 2. A rather drawn out wave is again observed at $E_{1/2} \approx -0.66$ V vs. *sce*; the plateau is poorly defined and although currents in this potential region are weakly dependent on solution velocity, they are significantly lower than expected for mass transport control.

3.2 *Constant potential electrolysis in the reticulated vitreous carbon cell*

A large number of controlled potential electrolyses were carried out in the flow cell with a reticulated vitreous carbon cathode on solutions of the deoxygenated sodium salt, pH 2, containing a low initial concentration of Pb(II). The lead concentration (by atomic absorption spectroscopy), the current and the charge passed were monitored as a function of time. The volume of solution recycled through the catholyte compartment was 3 litres for NO_3^- and SO_4^{2-} solutions and 2 litres for Cl^-, ClO_4^- and BF_4^-. The electrolyses were conducted at potentials in the "plateaux" regions of the *I–E* curves described.

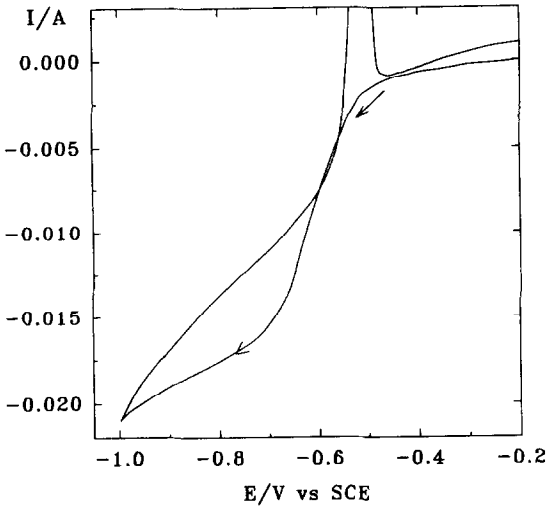

Fig. 6. Current-potential curve for saturated Pb(II) in 0.5 M Na_2SO_4 at pH 2 at a 60 ppi reticulated vitreous carbon cathode. The linear flow velocity is 0.21 m s^{-1}. Potential scan rate 5 mV s^{-1}. Temperature 298 K.

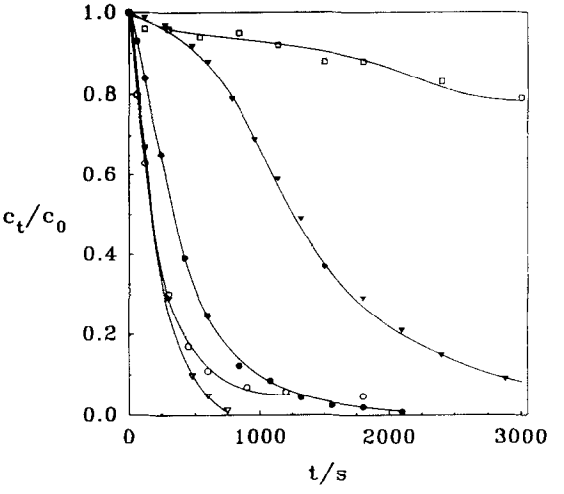

Fig. 8. Plots of normalised concentration, c_t/c_0, of Pb(II) vs. t for a 60 ppi reticulated vitreous carbon cathode in the media (▽) 0.5 M NaCl, (○) 0.5 M $NaClO_4$, (●) 0.5 M $NaBF_4$, (▼) 0.5 M $NaNO_3$, (□) 0.5 M Na_2SO_4 all pH 2. Potentials −0.8 to −0.9 V vs. *sce*. Initial solution ≈ 10 ppm Pb(II). Linear velocity 0.088 m s^{-1} (flow rate 0.053 dm^3 s^{-1}). Temperature 298 K.

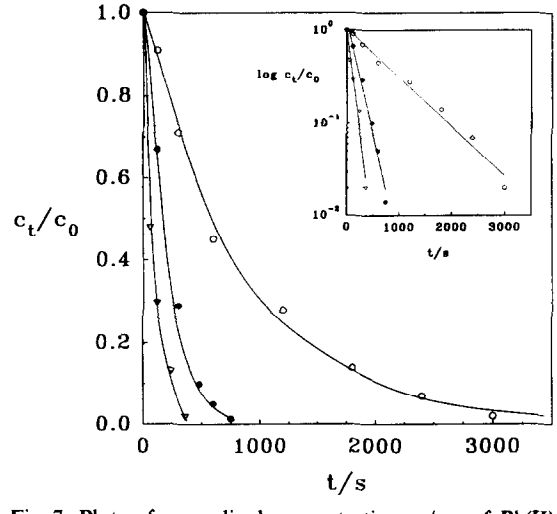

Fig. 7. Plots of normalised concentration, c_t/c_0, of Pb(II) vs. t. Initial solution 10 ppm Pb(II) in 0.5 M NaCl, pH 2. Reticulated vitreous carbon cathode: (○) 10 ppi, (●) 60 ppi, (▽) 100 ppi. Linear velocity 0.088 m s^{-1} (flow rate 0.053 dm^3 s^{-1}). The inset shows the same data presented as log c_t/c_0 vs. t. Temperature 298 K.

Table 2. Figures of merit for three grades of RVC material. Linear flow velocity 0.088 m s^{-1} (flow rate 0.053 dm^3 s^{-1}). 298 K. The normalised space velocity s_n is the volume of solution for which 90% of the Pb(II) may be removed in unit time by unit volume of electrode. E_v^n is the energy required to remove 90% of the Pb(II) from unit volume of solution

Electrode /ppi	$[Pb(II)]_{initial}$ /ppm	s_n /m^3 m^{-3} h^{-1}	E_v^n Wh m^{-3}
10	9	120	9.2
60	10	500	5.8
100	10	860	6.8

Figure 7 shows the decay with time of the normalised lead ion concentration in solution during electrolyses carried out with cathodes fabricated from the three grades of reticulated vitreous carbon; the medium was 0.5 M NaCl, pH 2 and the lead concentration was 9–10 ppm at the beginning of the electrolysis. In each case the potential was −0.9 V vs. *sce* where the previous experiments demonstrated that the lead deposition was mass transport controlled. With each of the reticulated vitreous carbons, the Pb(II) concentration could be reduced to below 0.2 ppm with a good overall current efficiency, 50% with the 10 ppi electrode and 70% for both 60 and 100 ppi materials. It can be seen from Fig. 7 that the decay in concentration becomes more rapid with an increase in the ppi of the reticulated vitreous carbon. The decays also appear to be exponential with time and this could be confirmed by plotting log c_t/c_0 vs. t, see the inset in Fig. 7. In fact, the decay is linear over two decades change in Pb(II) concentration. Modelling the system (cell + reservoir) as a simple batch process where all the electrode surface is operating under mass transfer control, the concentration should decay according to the equation

$$\log \frac{c_t}{c_0} = -2.3 \frac{k_m A_e V_e}{V_T} t \qquad (2)$$

where c_t and c_0 are the concentrations of Pb(II) at time t and the beginning of the electrolysis respectively and V_T is the volume of the solution being electrolysed. Hence, the slope of the log c_t/c_0 vs. t plots may be used to estimate further values of $k_m A_e$. The values calculated are some 20–30% higher than those determined from the I–E curves at the same flow rates and this may well result from surface roughness created by the deposition of the lead.

Table 3. Comparison of the performance of electrolyses for the removal of Pb(II) in different electrolyte, all 0.5 M at pH 2. Reticulated vitreous carbon, 60 ppi electrode. Electrolyte velocity 0.088 m s^{-1} (flow rate 0.053 dm^3 s^{-1}). 298 K. Note that in sulfate solution, the electrolysis never reached 90% depletion and the data in parentheses indicate the electrolysis time and the current efficiency at this point

Media	E/V	$[Pb(II)]_{t=0}$ /mM	$[Pb(II)]_{end}$ /mM	t for 90% removal/s	I_{EFF} for 90% removal
NaCl	−0.9	10	0.1	480	80
$NaNO_3$	−0.6	90	0.5	2500	80
$NaClO_4$	−0.9	10	0.4	600	50
$NaBF_4$	−0.9	12	0.1	1000	50
Na_2SO_4	−0.85	10	8.5	(3600)	(8)

It can be seen that the reticulated vitreous carbon cathodes perform well in the chloride medium. The removal of Pb(II) is both rapid and efficient. Table 2 compares the normalised space velocity, s_n, and the energy consumption for 90% removal of the Pb(II), E_v^n. Both figures of merit confirm the excellent performance of these electrodes; as expected, the 100 ppi material performs best.

Figure 8 shows Pb(II) concentration decay curves in each of the five electrolytes for electrolyses carried out with a 60 ppi cathode at potentials in the range −0.8 to −0.9 V. For perchlorate, tetrafluoroborate and nitrate media, the Pb(II) concentration drops smoothly with time to < 1 ppm although the rate of decay is not as rapid as with a chloride medium; this again implies that the lead deposition reaction from these solutions is not mass transport controlled. Particularly, the curve for nitrate medium shows a well defined initial period during which little Pb(II) is removed and thereafter the process accelerates; this is fully consistent with the I–E and I–t responses for this solution. From sulfate solution, the removal is, however, much slower and there was no definitive evidence that the concentration of lead could be reduced to low levels. Moreover, the currents are considerably lower than in the other media and the current efficiency is always very poor. The comparison between media is made again in Table 3. Here the rate of removal is compared using the time required for the removal of 90% of the Pb(II) from solution; this time increases along the series $Cl^- < ClO_4^- < BF_4^- < NO_3^-$ while this level could not be achieved from sulfate. The table also shows that in the media other than sulfate, the Pb(II) level could also be reduced to below < 1 ppm. In fact, the $[Pb(II)]_{end}$ are the concentrations when the electrolyses were terminated and we believe that it would be possible to bring down the Pb(II) concentration to ≪0.1 ppm with further electrolysis. It should also be noted that in the media other than sulfate, the current efficiencies are good although, as expected, the current efficiency decreased as the Pb(II) concen-

Table 4. Cathodic and anodic charges during the deposition and dissolution of Pb(II) on a 60 ppi electrode in 0.5 M Na_2SO_4 pH 2. The potential was held at the value shown for τ s and then scanned to positive potentials at 5 mV s^{-1}. [Pb(II)] = 10 ppm. Linear flow velocity 0.088 m s^{-1} (flow rate 0.053 dm^3 s^{-1}). The theoretical charge, q_T, calculated from equation (1) using k_mA_e values of 0.2, 0.39 and 0.66 s^{-1} for 298, 313 and 333 K, respectively. The charge for the removal of all the Pb(II) in solution is 35 C

	Deposition time, τ/s											
	$\tau = 20$				$\tau = 100$				$\tau = 1000$			
E/V vs. *sce*	q_C/C	q_A/C	q_A/q_C	q_C/q_T	q_C/C	q_A/C	q_A/q_C	q_C/q_T	q_C/C	q_A/C	q_A/q_C	q_C/q_T
T = 298 K		q_T = 1.1 C				q_T = 5.1 C				q_T = 24.2 C		
−0.6	0.13	0.09	0.70	0.11	0.28	0.16	0.6	0.05	1.7	0.4	0.25	0.07
−0.8	0.65	0.19	0.29	0.57	1.2	0.25	0.22	0.22	5.7	0.47	0.08	0.23
−1.2	2.0	0.32	0.16	1.77	2.8	0.36	0.13	0.54	10	1.8	0.17	0.43
−1.4	5.0	0.32	0.06	4.42	7.8	0.84	0.11	1.5	37	1.6	0.04	1.5
−1.6	8.1	2.1	0.25	7.17	15	2.6	0.16	3.0	75	8.9	0.11	3.1
T = 313 K		q_T = 2.1 C				q_T = 9.0 C				q_T = 27.4 C		
−0.6	0.21	0.11	0.52	0.1	0.49	0.24	0.5	0.05	3.1	0.91	0.29	0.11
−0.8	1.24	0.31	0.25	0.6	1.9	0.50	0.26	0.22	9.4	1.0	0.11	0.34
−1.2	4.3	0.72	0.17	2.0	5.6	0.90	0.16	0.62	22	3.7	0.17	0.79
−1.4	7.4	0.12	0.02	3.5	12	1.2	0.09	1.4	62	2.6	0.04	2.2
−1.6	16	4.9	0.30	7.5	23	6.5	0.28	2.6	120	18	0.15	4.4
T = 333 K		q_T = 3.4 C				q_T = 14 C				q_T = 29 C		
−0.6	0.36	0.24	0.67	0.1	0.77	0.37	0.50	0.05	5.1	0.62	0.12	0.2
−0.8	1.7	0.50	0.29	0.5	2.7	0.52	0.19	0.2	11	1.6	0.14	0.4
−1.2	4.9	1.0	0.20	1.4	6.7	1.3	0.19	0.5	29	4.5	0.15	1.0
−1.4	14	2.6	0.18	4.1	21	1.7	0.07	1.5	114	6.8	0.06	3.9
−1.6	18	4.4	0.24	5.4	44	8.8	0.20	3.1	280	22	0.08	9.7

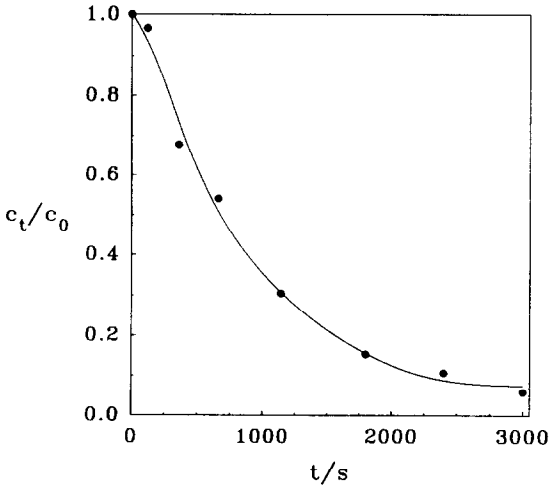

Fig. 9. Plot of normalised concentration, c_t/c_0, of Pb(II) vs. t for a 60 ppi reticulated vitreous carbon cathode in 0.5 M Na_2SO_4, pH 2. Initial solution is 14 ppm Pb(II). Linear velocity 0.088 m s^{-1} (flow rate 0.053 dm^3 s^{-1}). Potential −1.40 V vs. *sce*. Temperature 333 K.

tration drops below a certain level. Electrolyses were also carried out with 10 and 100 ppi reticulated vitreous carbon and the results were similar; in all media except sulfate, the rate of electrolysis increased with the number of ppi. With sulfate solutions the extent of Pb(II) removal was always poor.

3.3 *Further experiments with sulfate medium*

In view of the poor results achieved in the sulfate solution, several further experiments were carried out. The potential of a 60 ppi reticulated vitreous carbon electrode was held for a fixed time (τ = 20, 100 or 1000 s) at a potential negative to that where lead deposition was expected and then the potential was scanned at 5 mV s^{-1} towards positive potentials where lead dissolution was observed as an anodic stripping peak. These experiments were carried out at three temperatures. In each experiment the cathodic charge during the potential hold. q_C, and the anodic charge under the stripping peak, q_A, were measured. Table 4 reports these charges as well as the ratios, q_A/q_C and q_C/q_T where q_T is the theoretical charge passed assuming that the deposition of lead is mass transport controlled throughout the potential hold. This was estimated using equation (1) to calculate the change in concentration of Pb(II) concentration during the period $t = \tau$ and using Faraday's law to calculate the required charge.

The data show several interesting trends: (i) at low negative potentials, the cathodic charge is always low compared to q_τ and hence the deposition cannot be mass transport controlled; it is not until potentials where competing reactions, particularly H_2 evolution, become important that q_C/q_T approaches and then exceeds one, (ii) at low negative potentials and short deposition times, q_A/q_C is quite high so much of the cathodic charge is due to metal deposition, (iii) on the other hand, at low negative potentials and longer deposition times, q_A/q_C decreases and it appears that lead deposition is poisoned, perhaps by the formation of a poorly conducting layer of a lead salt, (iv) at the very negative potentials and particularly at elevated temperatures, however, the situation changes. Although $q_C/q_T \gg 1$ due to H_2 evolution, it is certain that deposition of lead starts to occur at a rate which is significant compared to mass transport control. This may be deduced by comparing q_A and q_T and, in fact, in some experiments $q_A > q_T$ and this may only be explained due to an enhancement of mass transport of Pb(II) by the evolving gas bubbles. These comments all assume that the lead on the surface of the reticulated vitreous carbon is all dissolved anodically during the slow potential sweep. This will only be the case if the deposit has a high area; thus a polished bulk lead electrode passivates rapidly with a layer of lead sulfate while, in contrast, the negative electrode of a lead acid battery fabricated from a paste will discharge very significantly). In the experiments of Table 4, there is no certainty that all the lead dissolves anodically and then the measured values of q_A would underestimate the amount of lead deposition. On the other hand, in some experiments, q_A approaches the value expected for mass transport controlled deposition and, hence, very significant lead dissolution must be taking place.

Overall, there can be no doubt that at the very negative potentials, the fraction of Pb(II) removed from solution increases markedly. This suggests that further Pb(II) species in solution become electroreducible at these potentials although, in these rather extreme conditions. This is consistent with the smaller than expected wave in the I–E curve for sulfate solution. Alternatively, it could be proposed that some Pb(II) is removed as $Pb(OH)_2$ due to an increase in pH at the electrode surface due to H_2

Table 5. The removal of Pb(II) from 0.5 M sodium sulfate, pH 2. 60 ppi reticulated vitreous carbon cathode. Electrolyte linear velocity 0.088 m s^{-1} (flow rate 0.053 dm^3 s^{-1})

$-E$ vs. *sce*/V	$[Pb]_{initial}$/ppm	$[Pb]_{end}$/ppm	% depletion	I Efficiency /%	Time for 90% depletion
T = 298 K					
1.3	7.0	6.5	7	4	—
1.5	9.0	0.6	93	18	2400
1.7	7.0	0.5	93	14	2000
T = 333 K					
1.2	14	9	35	15	—
1.4	14	0.3	97	13	2500
	7.0	0.2	97	8	3000

evolution in these conditions of high current density but this would not be consistent with the large anodic stripping charges which were observed. In any case, these results encouraged us to carry out some electrolyses using a 60 ppi reticulated vitreous carbon cathode at very negative potentials. A typical lead depletion curve is shown in Fig. 9 and some other data are reported in Table 5. It can be seen that the lead is, indeed, removed from solution under these conditions. The removal of Pb(II) was, however, slower than expected, *eg*, 90% depletion of the Pb(II) is achieved in 2000–2500 s (compared to 80 s for a mass transport controlled reaction at 333 K). Also the current during the electrolyses are high so that the current efficiency is only moderate.

4. DISCUSSION

It has been shown that in all five solutions at pH 2, it is possible to remove Pb(II) from solution using the flow cell with a reticulated vitreous carbon cathode. Moreover, from a technical viewpoint, the Pb(II) can be decreased to the level necessary for discharge of effluent into rivers and the sea with an acceptable current and energy efficiency. On the other hand, the conditions which must be employed depend to a surprising extent on the anion present in the medium. Only with the chloride solution was the deposition of lead simply mass transport controlled.

In nitrate, perchlorate and tetrafluoroborate solutions, removal of Pb(II) was possible but the rate of removal was always slower than predicted from models which assume mass transport control. Moreover, *I–E* potential curves recorded at the reticulated vitreous carbon materials were complex and there was important hysterisis between forward and back scans. Moreover, the exact form of the response varied with the history of the electrode. These observations imply that there were slow steps in the nucleation and/or early growth of the lead deposit on this carbon surface and this interpretation could be confirmed by potential step experiments. It should be noted, however, that these kinetic limitations are not general to all carbon surfaces. For example, cyclic voltammograms as well as rotating disc experiments carried out with a polished vitreous carbon disc electrode did not show the complications; in all solutions, steep reduction peaks/waves of the height expected for mass transport control were observed on the forward sweep. Indeed, the responses had all the features characteristic of rapid nucleation and growth and a fast Pb(II)/Pb couple. Hence, the slow steps in the early stages of deposition are determined by characteristics of the reticulated vitreous carbon surface and this suggests that modification or pretreatment of the surface may accelerate deposition from these solutions. It was further noted above that the addition of chloride ion to the solutions appeared to catalyse deposition. Mostany *et al.*[27] have reported a detailed study of lead deposition onto vitreous carbon from halide media and conclude that while the kinetics of growth do not change, the number of nuclei increases with halide concentration; this, of course, will change the deposit characteristics. They interpretted this conclusion in terms of halide ion adsorption on the carbon surface at potentials where the deposition of lead commences and consequent coadsorption of Pb(II) species on the surface which are the precursors to lead nuclei. Such coabsorption of metal ions in the presence of adsorbable anions has been demonstrated at mercury surfaces[28, 29]. In contrast, nitrate, perchlorate and tetrafluoroborate are all non-complexing anions and anions which are unlikely to adsorb significantly on the surface. Certainly, the addition of trace chloride ion (if it is not already present in solution) may be one approach to improving the performance of processes for the removal of Pb(II) from such solutions.

In the sulfate solution, the problems seem to arise from different complications. It appears that not all the Pb(II) in solutions is electroactive at potentials positive to those where H_2 evolution commences. Furthermore, if deposition is carried out at a potential in the plateau of the reduction wave observed in the *I–E* curves, the deposition starts readily but then the surface poisons; this is most likely to be due to the formation of a passivating layer. Fortunately, it is possible to achieve the required level of removal by operating at more negative potentials. It is also advantageous to carry out the electrolyses out at elevated temperatures, *eg*, 333 K. Although lead deposition is then accompanied by considerable H_2 evolution, the current efficiency remains acceptable even if lower than can be achieved with the other solutions.

A recent survey[30] of the waste stream from three lead acid battery manufacturers found that it typically had a pH in the range 1.6–2.9 and the soluble lead content was 5–15 ppm. Moreover, the state of the art precipitation technology using Fe(III) and NaOH was able to reduce this Pb(II) level to below 0.2 ppm. Therefore, we believe that the electrolytic treatment using a reticulated vitreous carbon cathode could be applied directly to this waste stream and it can also decrease the Pb(II) level at least to the same concentration, suitable for direct discharge to the sewer.

REFERENCES

1. F. Goodridge and A. R. Wright, in *Comprehensive Treatise of Electrochemistry, Volume 6*, (Edited by J. O'M. Bockris, B. E. Conway, E. Yeager and R. E. White), p. 393, Plenum (1983).
2. D. Pletcher and F. C. Walsh, in *Electrochemistry for a Cleaner Environment*, (Edited by J. D. Genders and N. L. Weinberg) p. 51, The Electrosynthesis Co (1992).
3. F. C. Walsh and G. W. Reade in *Environmental Orientated Electrochemistry*, (Edited by C. A. C. Sequeira) p. 3, Elsevier (1994).
4. D. Pletcher and F. C. Walsh, *Industrial Electrochemistry*, Chapman & Hall (1990).
5. F. C. Walsh, *A First Course in Electrochemical Engineering*, The Electrochemical Consultancy (1993).
6. J. Wang, *Electrochim. Acta* **26**, 1724 (1981).
7. A. N. Strohl and D. J. Curran, *Anal. Chem.* **51**, 353 (1959).
8. A. N. Strohl and D. J. Curran, *Anal. Chem.* **51**, 1045 (1979).
9. A. N. Strohl and D. J. Curran, *Anal. Chem.* **51**, 1050 (1979).

10. W. J. Blaedel and J. Wang, *Anal. Chem.* **51,** 799 (1979).
11. W. J. Blaedel and J. Wang, *Anal. Chem.* **51,** 1724 (1979).
12. W. J. Blaedel and J. Wang, *Anal. Chem.* **52,** 76 (1980).
13. J. Wang and H. Dewald, *Anal. Chim. Acta* **136,** 77 (1982).
14. J. Wang and H. Dewald, *J. electrochem. Soc.* **130,** 1814 (1983).
15. D. Pletcher, I. Whyte, F. C. Walsh and J. P. Millington, *J. appl. Electrochem.* **21,** 659 (1991).
16. D. Pletcher, I. Whyte, F. C. Walsch and J. P. Millington, *J. appl. Electrochem.* **21,** 667 (1991).
17. D. Pletcher, I. Whyte, F. C. Walsh and J. P. Millington, *J. Chem. Tech. Biotechnol.* **55,** 147 (1992).
18. D. Pletcher, I. Whyte, F. C. Walsh and J. P. Millington, *J. appl. Electrochem.* **23,** 82 (1993).
19. P. Tissot and M. Fragniere, *J. appl. Electrochem.* **24,** 509 (1994).
20. C. Ponce de Leon and D. Pletcher, *J. appl. Electrochem.* **25,** 307 (1995).
21. I. Whyte, Ph.D. Thesis, University of Southampton, 1990.
22. S. Langlois and F. Coeuret, *J. appl. Electrochem.* **19,** 43 (1989).
23. Data sheet, Energy Research and Generation, Oakland, CA.
24. *International Critical Tables of Numerical Data in Physics, Chemistry and Technology*, (Edited by E. W. Washburn) McGraw Hill (1929).
25. C. J. Brown, D. Pletcher, F. C. Walsh, J. K. Hammond and D. Robinson, *J. appl. Electrochem.* **24,** 95 (1994).
26. J. Mostany, J. Parra and B. Scharifker, *J. appl. Electrochem.* **16,** 333 (1986).
27. M. Sluyters-Rehbach, J. S. M. C. Breukel, K. A. Gijsbertsen, C. A. Wijnhorst and J. H. Sluyters, *J. electroanal. Chem.* **38,** 17 (1972).
28. D. J. Barclay and F. C. Anson, *J. electroanal. Chem.* **28,** 71 (1970).
29. A. Montillet, J. Comiti and J. Legrand, *J. appl. Electrochem.* **24,** 27 (1994).
30. G. Macchi, M. Pagano, M. Santor and G. Tiravanti, *Water Res.* **27,** 1511 (1993).